

# Chapter 5

---

## Determining the physical interactions within the zebrafish Jam family

### Summary

In this chapter I describe the biochemical interactions between the soluble ectodomains of all identified members of the zebrafish Jam family and the implications for studying Jam family interactions during development in light of their spatio-temporal expression data. The cloned extracellular domain of each of the Jam family members was expressed by transient transfection of a mammalian cell line, purified and used in a surface plasmon resonance (SPR) -based biochemical interaction screen. The dissociation rate constants for each monomeric interaction was determined from the dissociation phase data and used to compare their relative strengths. Interactions amongst the Jam family members appear to be conserved between fish, mice and humans. The wide range of interaction strengths suggests that even closely related family members would be less able to act redundantly. In the context of spatio-temporal expression in early development, only heterophilic interactions between Jamb and Jamc seem likely, given co-expression in fast muscle myoblasts.

## 5.1 Introduction

Interactions between mammalian JAM family members have already been described (figure 5.1; reviewed in Weber *et al*, 2007), though rarely in a systematic or quantitative way. Crystallographic studies have suggested two different binding modes between mouse and human JAM-A ectodomains; homophilic binding *in cis* through conserved residues in the surface formed by GFCC'  $\beta$ -strands, and homophilic binding of homodimers *in trans*. A bioinformatic analysis of the zebrafish Jam family showed strong conservation of the putative binding site in the membrane-distal immunoglobulin-like domain in all homologues (see Chapter 3), suggesting similar binding capabilities. I sought to test whether biochemical interactions were conserved in the zebrafish Jam family and to evaluate the likelihood of other Jam family interactions with either Jamb or Jamc that might confound functional studies. In order to achieve these goals, I undertook a systematic and comparative surface plasmon resonance interaction study using soluble ectodomain fragments of each Jam family member.

Surface plasmon resonance (SPR) is a very sensitive method to detect physical interactions between an immobilised ligand and a soluble analyte in real-time (reviewed in van der Merwe and Barclay, 1996; figure 5.2). Under total internal reflection, light reflecting off a thin conducting film at the interface between two media with different refractive indices will generate an electrical field. This evanescent wave field has a very limited depth of penetration across the media. At a certain combination of angle of incidence ( $\theta_i$ ) and wavelength ( $\lambda$ ), the incident light excites plasmons in the conducting film, resulting in a loss of reflected light at a corresponding angle of reflection ( $\theta_r$ ). Because the evanescent wave penetrates the media, the angle of incidence and wavelength necessary to cause this absorption of energy is dependent upon the refractive index of the media within the depth of penetration by the wave field. The Biacore technology uses sensor chips containing a thin film of gold (the conducting film) on a glass surface, over which a sample solution is passed by a microfluidic system. Changes in solute concentration within the depth of evanescent wave field change the refractive index of the media, and so the angle at which plasmons are excited in the gold film at a fixed wavelength (800 nm). The change in absorption angle is monitored in real time over a fixed range of  $\theta_i/\theta_r$  and recorded in arbitrary response units (RU). The ligand of interest is immobilised on the glass surface and analyte solutions are passed over the sample; any change in the SPR signal is recorded every tenth of a second (10 Hz, figure 5.3). An analyte that binds the immobilised ligand will change the SPR signal by changing

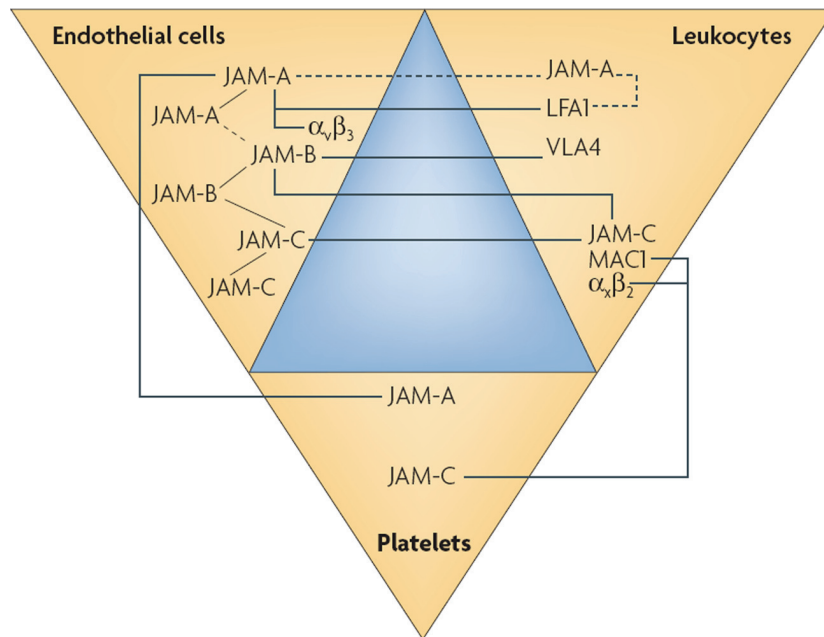


**Figure 5.1 Known extracellular interactions of JAM family proteins.**

Diagram illustrating known extracellular interactions between JAM family proteins and integrins expressed on the surface of mammalian endothelial and peripheral blood cells. Reproduced from Weber *et al* (2007), without permission.

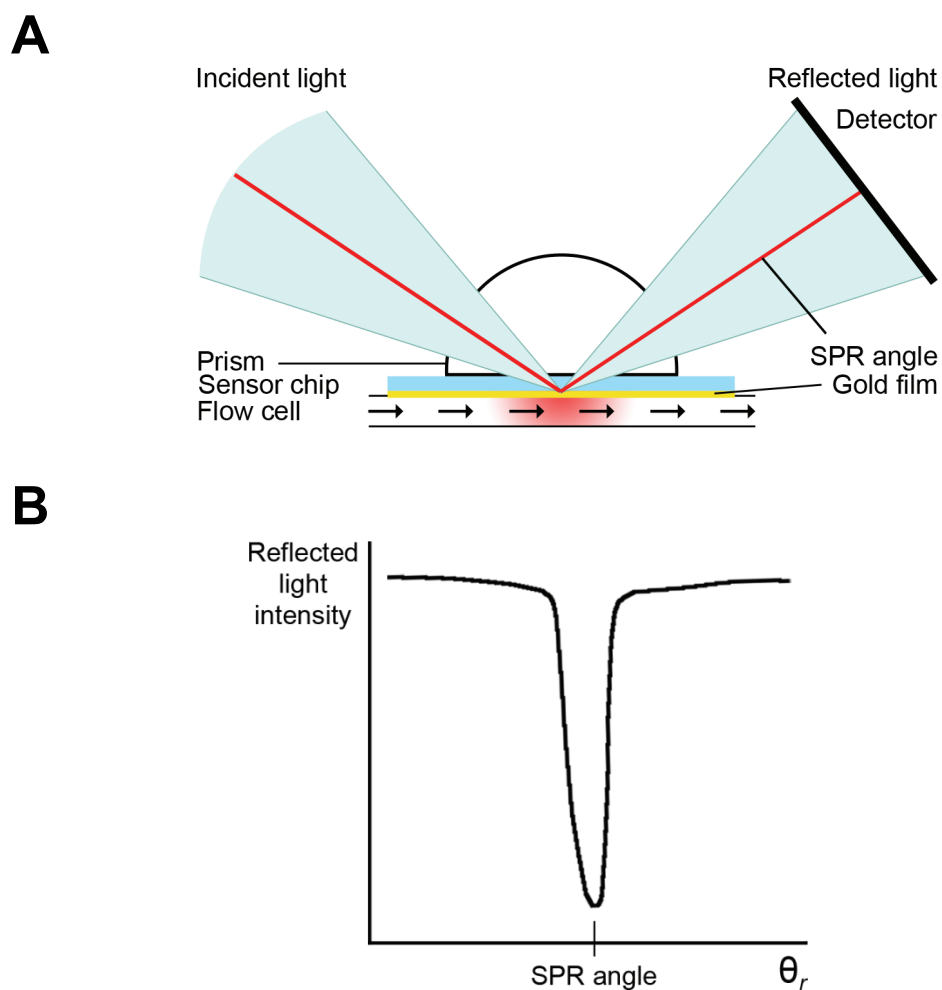
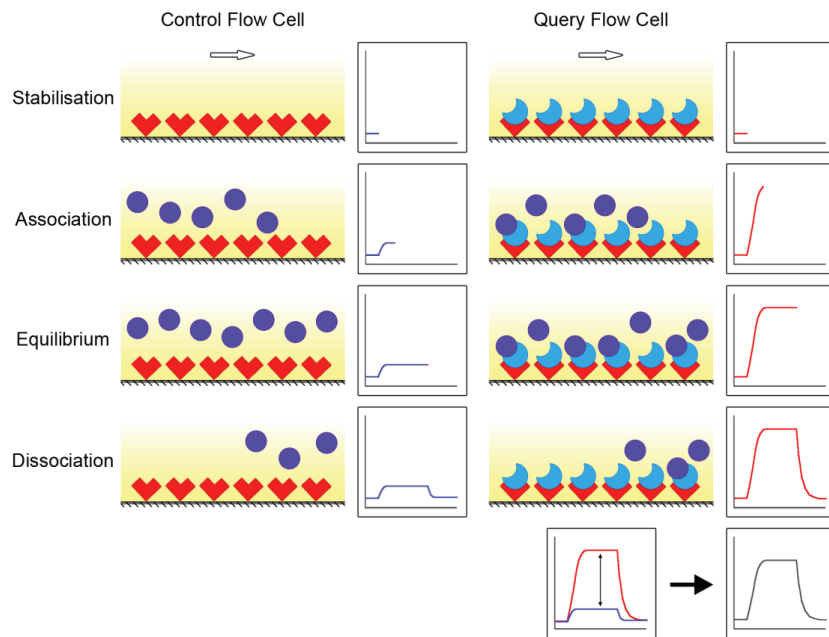


**Figure 5.2 The surface plasmon resonance principle.**

**A.** Schematic of Biacore technology used to detect protein interactions. Light ( $\lambda = 800 \text{ nm}$ ) at a fixed range of angle of incidence strikes a thin gold film, exciting plasmons and generating an evanescent wave field which penetrates the media within the flow cell. The light is reflected internally onto a detector which measures intensity. **B.** The intensity of reflected light drops at a particular angle that generates an evanescent wave field (the SPR angle). The SPR angle changes with respect to changes in the refractive index of the media passing through the flow cell. Modified from Biacore Sensor Surface Handbook, October 2003 edition, without permission.

**A**



**B**

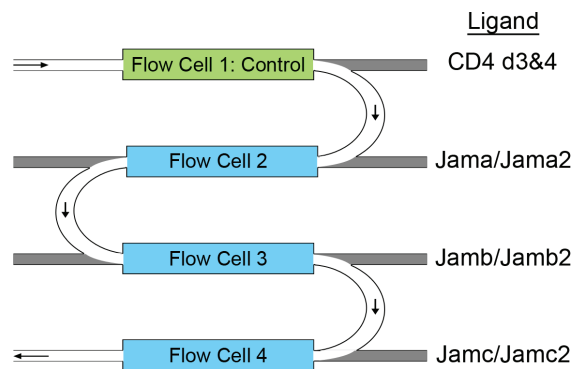


**Figure 5.3 Real-time monitoring of protein interactions by surface plasmon resonance.**

**A.** Schematic depicting real-time detection of interactions of an analyte (purple) with an immobilised ligand in a query flow cell (right, blue and red) but not in the control flow cell (left; red) in parallel over time: buffer stabilisation, association, equilibrium and dissociation (top to bottom). The changes in SPR responses plotted against time are displayed in the graphs to the right of each flow cell. Binding measurements are made by subtracting the control flow cell responses from the query cell responses. Arrows indicate the direction of flow. **B.** Schematic of the microfluidic chamber demonstrating arrangement of flow cells, the analyte flow path and the ligands immobilised in the flow cells of two sensor chips. A continuous flow of analyte allows each surface to be tested in parallel.

## Determining the physical interactions within the zebrafish Jam family

the refractive index of the media within the effective penetration depth of the evanescent wave field, approximately 20% of the wavelength of incident light (160 nm at  $\theta_i = 800$  nm). This increase in signal will be beyond the change in signal in the negative reference sample, tested in parallel. Binding is measured by subtracting the SPR response observed with the negative reference ligand from that observed with the query ligand. An analyte that doesn't bind the immobilised ligand will still change the SPR signal, as it has a different refractive index to the buffer used, but will not be beyond that observed in the negative reference.

The real-time monitoring of SPR signal allows for a quantitative analysis of the kinetics of binding. Comparing the half-lives of interactions is a useful and intuitive way to assess the relative strengths of similar binding events. For a simple interaction, the rate of decay of the interaction complex, assuming first-order dissociation kinetics, is defined as:

$$-\frac{d[A \cdot B]}{dt} = k_d [A \cdot B]$$

where  $[A \cdot B]$  is the concentration of the complex and  $k_d$  is the dissociation rate constant ( $s^{-1}$ ). At  $t = t_{1/2}$ , the concentration of the complex is halved:

$$\int_{[A \cdot B]}^{\frac{[A \cdot B]}{2}} \frac{d[A \cdot B]}{[A \cdot B]} = - \int_{t_0}^{t_{1/2}} k_d dt$$

After integration and subsequent rearrangement:

$$t_{1/2} = \frac{\ln 2}{k_d}$$

It is clear that the half-life depends on the dissociation rate constant ( $k_d$ ) alone. This is useful, because determining the true concentration of active protein within a sample is notoriously difficult, particularly if the protein is known to bind itself, and can introduce a considerable source of error. Note also that true first order dissociation produces a linear plot when the natural logarithm of concentration of bound complex is plotted against time:

$$\ln[A \cdot B] = -k_d \cdot t$$

with a slope equal to the inverse of the dissociation rate constant.

To assess the possibility of redundancy amongst zebrafish Jam family proteins I identified interactions amongst recombinant immunoglobulin domains using surface plasmon resonance. I identified many interactions with a range of strengths, suggesting little redundancy between the proteins with respect to biochemistry.

## 5.2 Jam family ectodomain production and purification

I tested all possible pairwise interactions amongst zebrafish Jam family proteins, using each protein as both immobilised ligand and soluble analyte. To do this, I expressed soluble recombinant ectodomains of each protein, fused to rat CD4 domains 3 and 4 (CD4-d3&4), in two forms using mammalian cell culture: one tagged with a C-terminal biotinylation peptide, the other with a C-terminal hexa-histidine tag (figure 5.4; see Materials and Methods for further details). The former were assessed by enzyme-linked immunosorbent assay (ELISA; figure 5.4) and immobilised on streptavidin-coated Biacore chips in molar amounts equivalent to the negative control ligand, CD4-d3&4 tag only (figure 5.3). The latter were purified using a nickel column, followed by gel filtration to remove impurities and exchange the protein into SPR buffer (figure 5.5). Analyte concentrations were estimated by absorbance at 280nm, based upon *in silico* predicted absorption co-efficients.

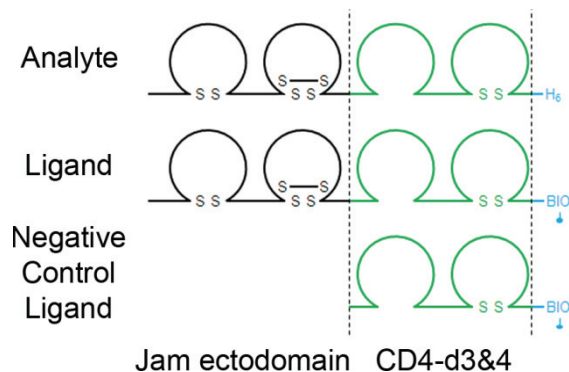
## 5.3 Using surface plasmon resonance to quantify Jam family interactions

To establish the network of interactions between the Jam family proteins, I performed an-all-against-all SPR screen using the recombinant proteins produced. After an analyte was purified, several dilutions were passed over each of the immobilised ligands at high flow rate to minimise re-binding effects. The SPR response in each flow cell was measured simultaneously and in real-time. The CD4-d3&4 tag negative control protein surface response was subtracted from the data collected in each flow cell in parallel and real-time. The data were corrected for a time lag in sample delivery between the flow cells which are connected in series (see Materials and Methods for full details; figures 5.3 and 5.6). Several biochemical interactions, of varying strengths, were identified within the family (figure 5.7).

## 5.4 Comparing Jam family interactions

To assess quantitative differences between interactions, I determined  $k_d$  and calculated half-lives from dissociation curves plotted from SPR data (tables 5.1 and 5.2). Each interaction was first shown to comply with first order dissociation kinetics by plotting the natural logarithm of specific binding against time (figure 5.8). Some interactions were not analysed because of limited data; where  $t_{1/2}$  is below the frequency of detection of the instrument used ( $\leq 0.1$  sec). Dissociation curves were then plotted for three different concentrations of analyte in each interaction and  $k_d$  estimated by fitting equations of the form:

**A**



**B**

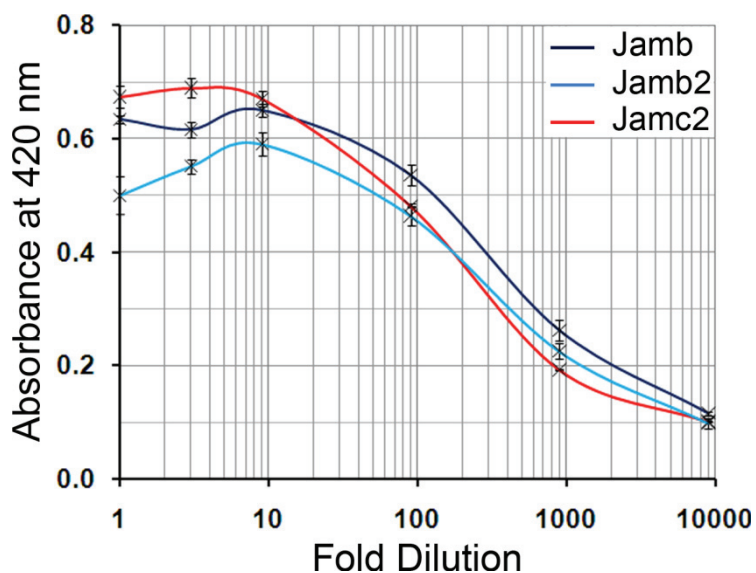


**Figure 5.4 Production and quantification of biotinylated Jam family ectodomains.**

**A.** Diagrams of fusion proteins produced for SPR screening. Jam ectodomains were fused to a CD4-d3&4 tag (green) and either a hexa-histidine tag ( $H_6$ ; analyte) or a substrate peptide for the biotin ligase, BirA (bio; ligand). The negative control ligand was the CD4-d3&4 tag and the BirA substrate peptide only. **B.** Example ELISA assay to quantify production of ligands tagged with biotin by BirA, using streptavidin-coated plates to capture the biotinylated protein.



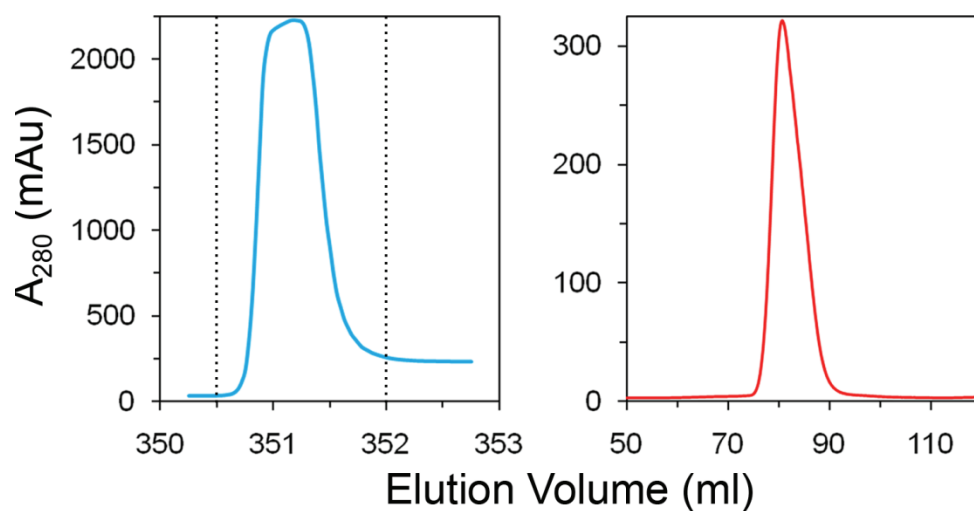


**Figure 5.5 Purification of histidine-tagged Jam family ectodomains.**

Example traces of purification of Jamc analyte by nickel column (left) followed by gel purification (right) as monitored by absorbance of flowthrough at 280 nm. The purified protein was eluted from a nickel column using imidazole and the combined peak fractions (dashed lines, left) were then purified by gel filtration (right). Peak fractions, eluted from the gel filtration column in SPR running buffer, were then used for SPR in serial dilutions.

## Determining the physical interactions within the zebrafish Jam family

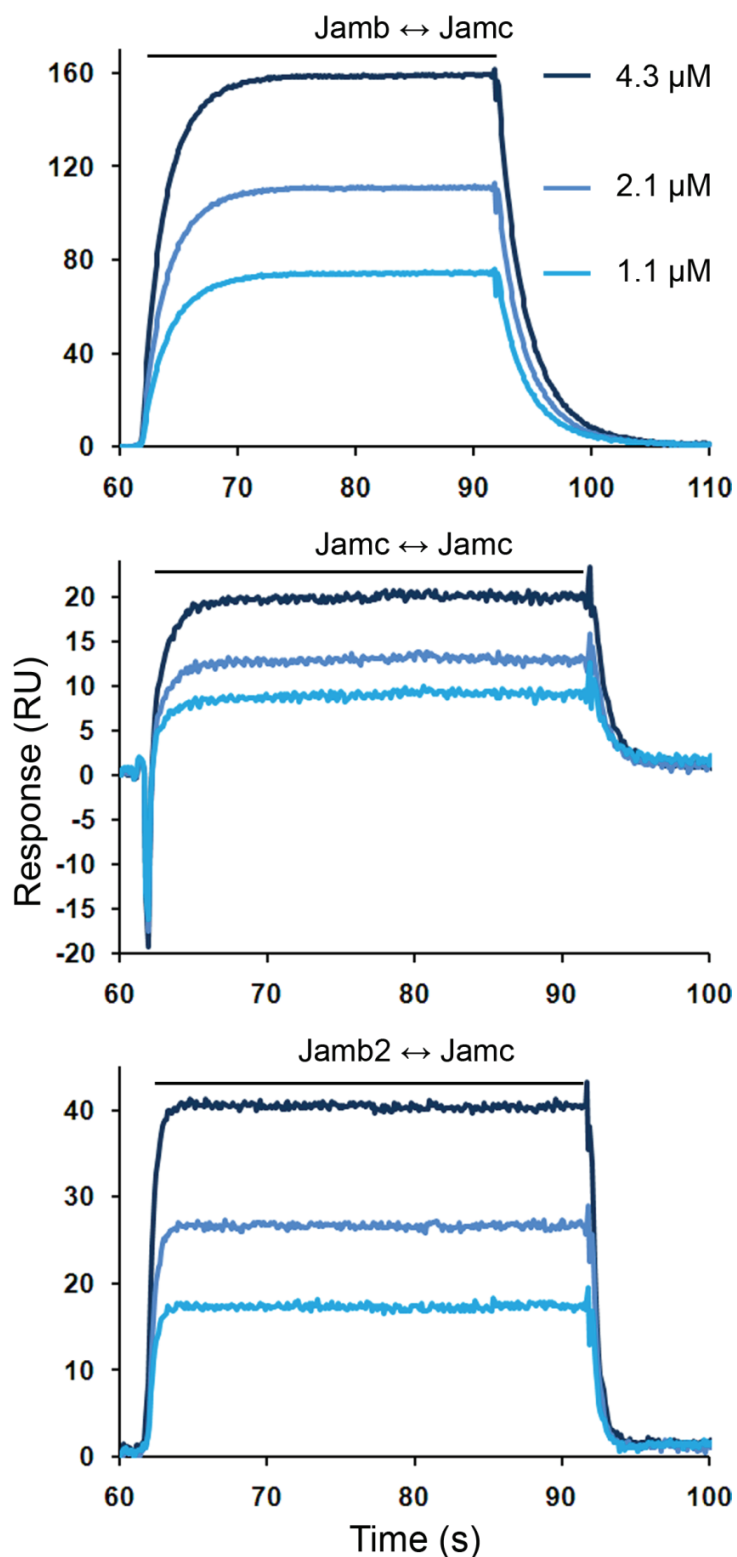


**Figure 5.6 Example sensorgrams of detected interactions.**

Sensorgrams demonstrating three interactions of differing affinity detected using the same analyte, Jamc, tested against immobilised Jamb, Jamc and Jamb2. Responses from experiments using three dilutions of analyte (4.2, 2.1 and 1.1  $\mu\text{M}$ ) are displayed for each interaction. Bar above sensorgrams represents injection phase.

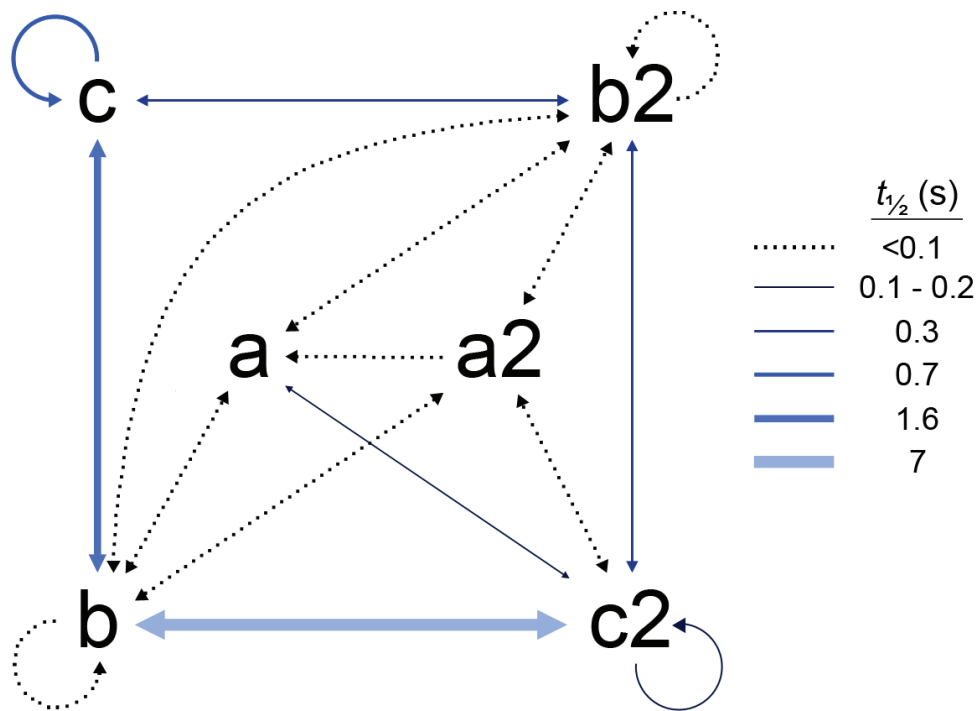


**Figure 5.7 Network of interactions detected between Jam family proteins.**

Schematic showing all interactions detected between Jam family extracellular domains in the surface plasmon resonance screen, colour-coded according to half-life. Double-headed arrows represent interactions detected in both orientations of immobilised ligand and analyte; single-headed arrows represent unreciprocated interactions.

**Table 5.1 Dissociation rate constants for interactions amongst JAM family proteins.** Dissociation rate constants are presented for each positive interaction observed. Interactions that were too weak to quantify are given the nominal value  $\geq 6.9$ , equivalent to a half-life of 0.1 seconds. Interactions that could be quantified are presented as a mean  $\pm$  S. D. (n = 3) and are highlighted in bold.

Ligand	Analyte					
	Jama	Jama2	Jamb	Jamb2	Jamc	Jamc2
Jama	-	-	$\geq 6.9$	$\geq 6.9$	-	<b><math>4.43 \pm 0.95</math></b>
Jama2	$\geq 6.9$	-	$\geq 6.9$	$\geq 6.9$	-	$\geq 6.9$
Jamb	$\geq 6.9$	$\geq 6.9$	$\geq 6.9$	$\geq 6.9$	<b><math>0.37 \pm &lt;0.01</math></b>	<b><math>0.09 \pm &lt;0.01</math></b>
Jamb2	$\geq 6.9$	$\geq 6.9$	$\geq 6.9$	$\geq 6.9$	<b><math>2.44 \pm 0.28</math></b>	<b><math>1.88^\dagger \pm 0.05</math></b>
Jamc	-	-	<b><math>0.50 \pm 0.04</math></b>	<b><math>2.86 \pm 0.22</math></b>	<b><math>1.03 \pm 0.09</math></b>	-
Jamc2	$\geq 6.9$	$\geq 6.9$	<b><math>0.11 \pm &lt;0.01</math></b>	<b><math>2.39^\dagger \pm 0.30</math></b>	-	<b><math>6.22 \pm 0.60</math></b>

† denotes an interaction that appears to display a two-phase dissociation - the dissociation rate constant is estimated from the first 0.9-1 seconds of dissociation (accounting for approximately 85-90% of specific binding) that fits a first order exponential decay model with an  $R^2 \geq 0.97$ .

**Table 5.2 Calculated half-lives for interactions amongst JAM family proteins.** Calculated half-lives are presented for each positive interaction observed. Interactions that were too weak to quantify are given the nominal value of  $\leq 0.1$  seconds. Half-lives are calculated using the average value of the dissociation rate constant for each interaction and the formula  $t_{1/2} = \ln 2/k_d$ .

Ligand	Analyte					
	Jama	Jama2	Jamb	Jamb2	Jamc	Jamc2
Jama	-	-	$\leq 0.1$	$\leq 0.1$	-	<b>0.16</b>
Jama2	$\leq 0.1$	-	$\leq 0.1$	$\leq 0.1$	-	$\leq 0.1$
Jamb	$\leq 0.1$	$\leq 0.1$	$\leq 0.1$	$\leq 0.1$	<b>1.87</b>	<b>7.70</b>
Jamb2	$\leq 0.1$	$\leq 0.1$	$\leq 0.1$	$\leq 0.1$	<b>0.28</b>	<b>0.37<sup>†</sup></b>
Jamc	-	-	<b>1.39</b>	<b>0.24</b>	<b>0.67</b>	-
Jamc2	$\leq 0.1$	$\leq 0.1$	<b>6.30</b>	<b>0.29<sup>†</sup></b>	-	<b>0.11</b>

<sup>†</sup> denotes an interaction that appears to display a two-phase dissociation – the half-life was calculated from the dissociation rate constant estimated from the first 0.9-1 seconds of dissociation (accounting for approximately 85-90% of specific binding) that fits a first order exponential decay model with an  $R^2 \geq 0.97$ .

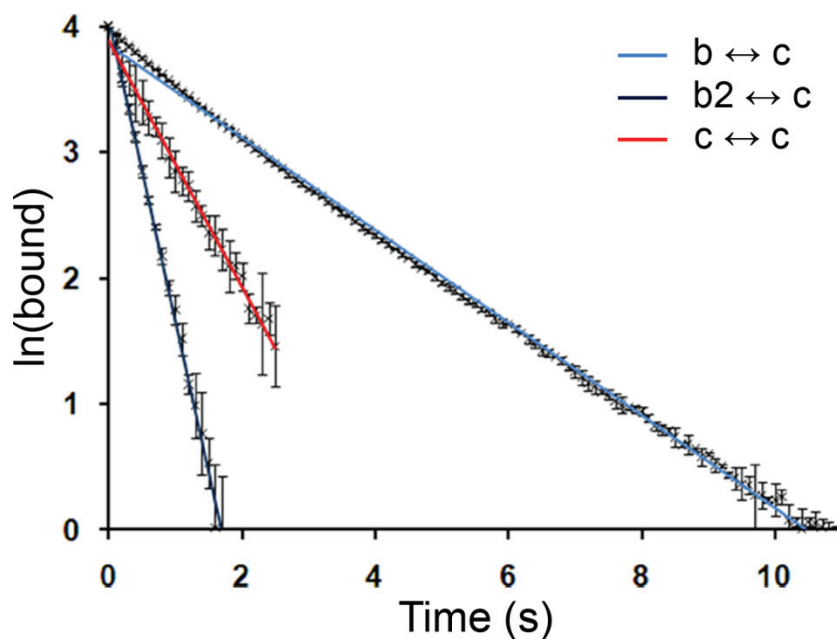


**Figure 5.8 Example plots of dissociation phase data demonstrating first-order kinetics.**

Three example plots of  $\ln(\text{bound})$  as a function of time for dissociation phase data of three interactions of differing affinity, demonstrating first-order dissociation kinetics. Each series represents the average of three experiments using different dilutions of Jamc analyte (4.2, 2.1 and 1.1  $\mu\text{M}$ ); error bars represent standard deviation.

$$y = Ae^{-k_d \cdot t}$$

to the data (figure 5.9, table 5.1). Estimates of  $k_d$  were then converted to half-lives, as previously described, and used for comparison (figure 5.9, table 5.2). A wide range of half-lives were determined, ranging from 7.7 seconds to 0.11 seconds. Estimates for  $k_d$  were slightly different depending on the orientation of ligand and analyte for a given interaction. This is likely to be because of rebinding effects, despite the high flow rate of analyte.

## 5.5 Discussion

To test the relative properties of each of the Jam family proteins I performed a quantitative all-against-all biochemical interaction screen using the conserved extracellular domains. The results described above demonstrate that the ectodomains do not appear to be biochemically equivalent with respect to binding kinetics or specificity *in vitro*.

The generalised scheme of protein interactions amongst family members seems to be conserved between zebrafish and mammals (compare figure 5.1 and figure 5.7). For example, zebrafish Jamb proteins interact with Jamc proteins. JAM-C is known to bind itself in mouse and human; similarly, each zebrafish JAM-C paralogue protein interacts homophilically. Some interactions have not been identified in previous studies, such as the weak interactions detected between Jamc2, JAM-B paralogues with both JAM-A paralogues. Curiously, Jamc and Jamc2 do not interact with each other, suggesting that they have diverged enough to no longer bind each other whilst retaining homophilic binding activity. Both JAM-C paralogue proteins also bind both Jamb proteins, with remarkably different affinities. In contrast, homophilic and heterophilic interactions were detected amongst Jamb proteins. Also, both Jamb paralogues were found to interact with Jama, but only one of the Jamc paralogues was found to, Jamc2. This suggests that whilst the JAM-C paralogues have diverged with respect to binding specificity, JAM-A and JAM-B paralogues have not, despite the high level of primary amino acid sequence conservation between the extracellular domains of paralogues in all 3 subgroups (see Chapter 3).

A defining characteristic of each of the JAM family proteins is a conserved binding site in the concave surface formed by the GFCC'  $\beta$ -strands of the distal immunoglobulin-like domain. This motif, R(V,I,L)E ... Y, contains residues important for forming salt bridges between monomers *in cis*, as identified by crystallographic studies (Kostrewa *et al*, 2001; Protá *et al*, 2003). The core of the motif is completely conserved amongst all JAM proteins from zebrafish to humans, but other amino

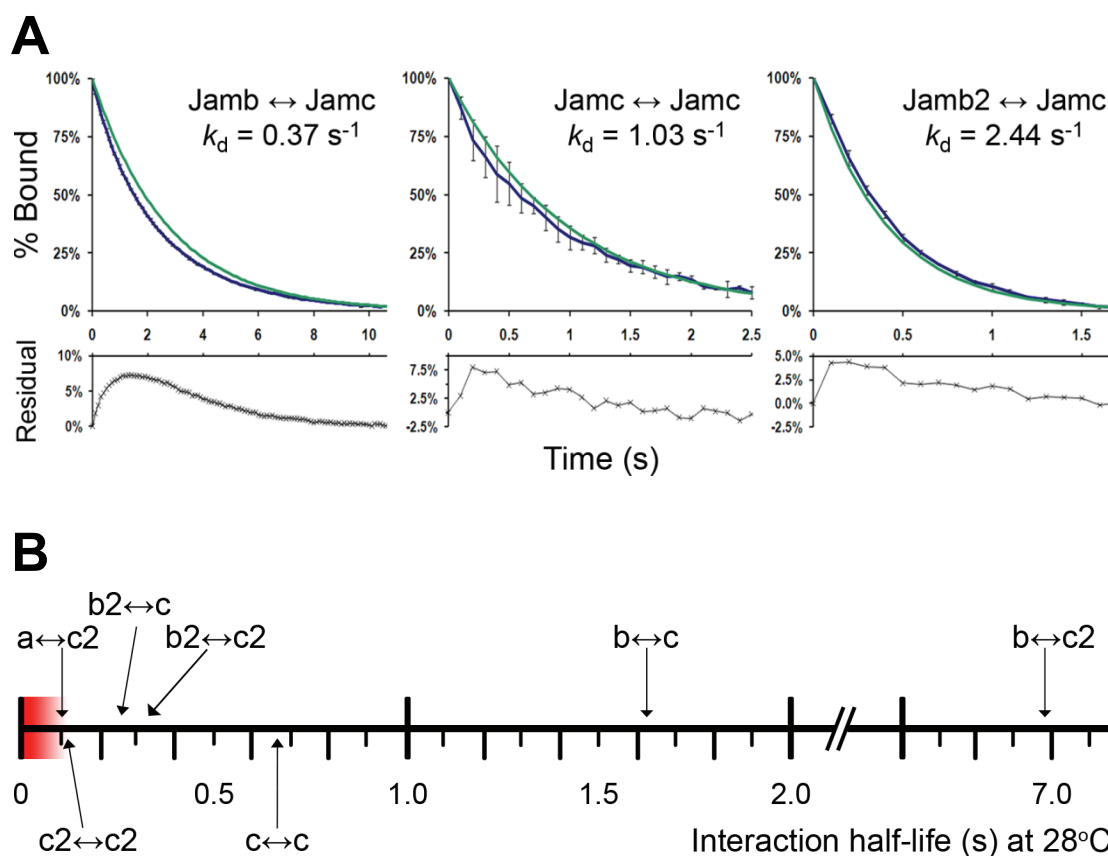


**Figure 5.9 Comparing dissociation phase data reveals a wide range of interaction strengths within the Jam family.**

**A.** Examples of observed dissociation curves (blue) and first order decay curves of the respective dissociation rate constants ( $y = Ae^{-k_d t}$ , green) demonstrating a goodness of fit for three interactions of differing strengths. Residuals represent the differences between observed and modelled data. Observed curves are the average of three experiments using different dilutions of Jamc analyte (4.2, 2.1 and 1.1  $\mu\text{M}$ ); error bars represent standard deviation. **B.** Scale showing the different half-lives for all interactions quantified; heterophilic interactions are grouped above the scale, homophilic interactions below. Region highlighted in red represents the detection limit of the instrumentation and materials used.



## Determining the physical interactions within the zebrafish Jam family

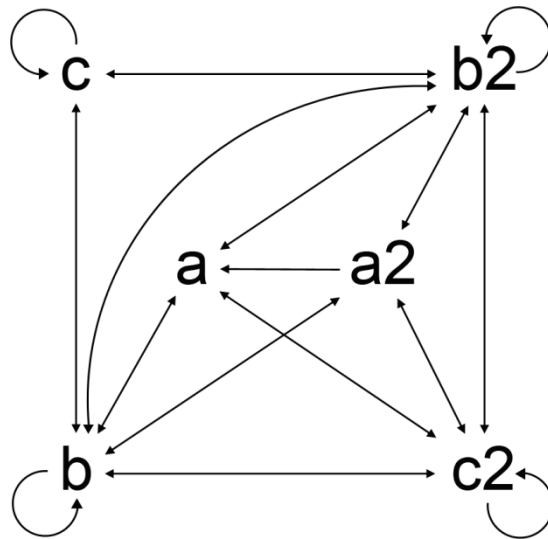
acids that form the binding surface are more variable. This comprehensive, quantitative study of the relative strengths of interactions demonstrates that there is great variability within the family. Crystallographic modelling suggests that the formation of dimers *in cis* through the GFCC' surface is necessary for interactions *in trans* (Kostrewa *et al*, 2001; Prota *et al* 2003). However, each of the dissociations I studied conformed to first-order kinetics, suggesting no pre-requirement of homodimer formation *in cis* for interactions *in trans*.

Unfortunately, many of the interactions identified were refractory to quantitative analysis, likely because of high  $K_D$  i.e. the analyte protein concentration was below that required to saturate available binding sites in each case. Detection of the weakest interactions could be improved by deliberate multimerisation of the extracellular domains through a C-terminal tag such as the cartilage oligomeric matrix protein (COMP). This would increase the avidity of any interaction and add confidence to the detection of weak interactions (Bushell *et al*, 2008). However, any kinetic data would be difficult to interpret or compare to other interactions, as association and dissociation phases would likely be of a higher order.

In summary, the data presented here suggest clear biochemical differences between the Jam family proteins with respect to binding specificity and kinetics, despite strong conservation of primary amino acid sequence. Intra-family interactions are broadly conserved, but paralogues demonstrate differing binding kinetics when interacting with the same ligand. These results suggest it is unlikely that any of the Jam family proteins function redundantly.



**A**



**B**

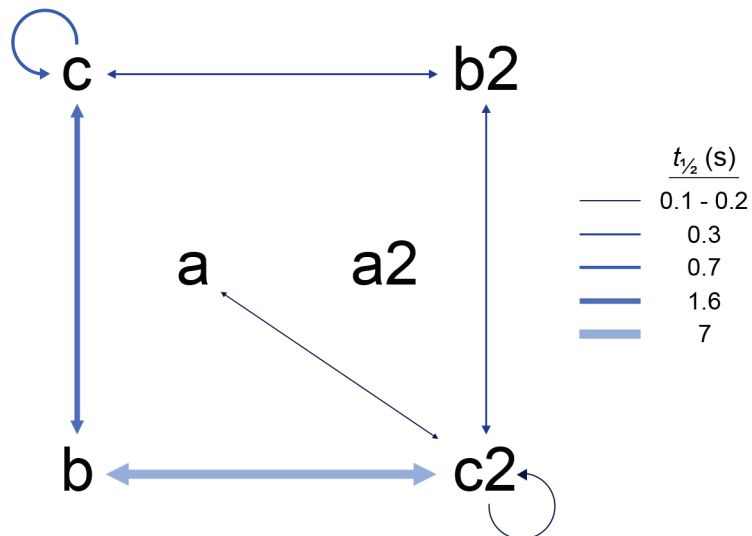


**Figure 5.7 Schematics of the interactions detected between Jam family proteins.**

**A.** Schematic showing all interactions detected between Jam family extracellular domains in the surface plasmon resonance screen. **B.** Schematic showing all quantified interactions, colour-coded according to half-life. Double-headed arrows